

**Proposed Design Method for EB-FRP Ties Debond Strain
Encompassing Short/Long and Thin/Thick Ties**

Junrui Zhang, Enrique del Rey Castillo, Ravi Kanitkar, Aniket D Borwankar, and Ramprasath R

Synopsis: A systematic literature review was conducted on pure tension strengthening of concrete structures using fiber-reinforced polymer (FRP), specifically for larger FRP tie applications. This work yielded a dataset of 1,627 direct tension tests, and highlighted the limitation of existing studies on studying thick and long FRP ties, which are typical in real construction scenarios. To overcome this shortcoming, 51 single lap shear tests were conducted on thicker and longer FRP ties, with the dimensions being 0.5 to 6 mm [0.02 to 0.24 in.] thickness, and 300 to 1,524 mm [12 to 60 in.] long. The critical parameters under consideration were concrete compressive strength, FRP thickness, and bond length. The findings demonstrate that thicker and therefore stiffer FRP ties have higher debond force capacity, while longer ties exhibit greater post-elastic deformation capacity but do not affect the debond force capacity. Concrete had a limited effect on either debond force or deformation capacity. A strength model is proposed for FRP systems under axial pure tension, which aligns well with both the published and tested results. This paper focuses on the development of design guidelines and codes to predict the debond strain for EB-FRP systems incorporating thicker and longer FRP ties, aiming to enhance the applicability of FRP to real-world construction scenarios.

Keywords: Externally bonded reinforcement (EBR), Fiber reinforced polymer (FRP), Reinforced concrete (RC), Interfacial bond behavior, Cohesive debonding, Single-lap shear test.

ACI student member **Junrui Zhang** is currently enrolled at the University of Auckland as a PhD candidate working on 'Seismic strengthening of floor diaphragms with carbon fiber composite materials (CFRP) ties'. Before that, Junrui completed his M.Phil. project in Structural Engineering at Lanzhou University with distinction. In the same period, he participated in an exchange program at the Swanson School of Engineering at the University of Pittsburgh.

ACI member **Enrique del Rey Castillo** is currently working at the University of Auckland as a Senior Lecturer, where he teaches and investigates concrete materials, design, and structures. His research interests include seismic behaviour and strengthening of existing concrete structures, mostly with FRP, and sustainability of concrete.

ACI member **Ravi Kanitkar** is currently working at KL Structures

ACI member **Aniket D Borwankar** is currently working at Simpson Strong-Tie

ACI student member **Ramprasath R** has recently completed the undergraduate studies in Civil Engineering at NIT Trichy and will be joining Virginia tech for fall 2023 to pursue master's in structural engineering. Research interest focuses on seismic strengthening of concrete structures.

INTRODUCTION

Application of externally bonded fiber-reinforced polymer (EB-FRP) is a widely used technique for retrofitting and strengthening existing structures. This technique involves bonding Fiber-Reinforced Polymer (FRP) materials such as glass, carbon, or aramid with an epoxy matrix to the external surface of the concrete structure. EB-FRP can provide improved resistance to flexural [1, 2], shear [3], and tension forces [4, 5], making it suitable for reinforcing various components such as beams [6], columns [7], walls [8], and floor diaphragms [9, 10]. Fig. 1 illustrates a regular FRP-strengthened concrete block under single-lap shear tests. The force transfer mechanism between the FRP and the concrete is the bond stresses provided by the epoxy resin, with the failure typically being related to the fracture of a shallow layer of concrete when subjected to tension and/or shear forces. In other words, neither the resin nor the fibers typically fail. Thus, the failure strain of the EB-FRP system is often much lower than the fracture strain of the FRP, due to the low tensile capacity of concrete. Current published studies predominantly focused on thin (< 0.5 mm [0.02 in.]) and short (< 300 mm [12 in.]) FRP ties (aka sheets), which are often not representative of real in-situ construction scenarios where thick and long FRP ties are typically used. This shortcoming is reflected in commonly used design guidelines. For example, Section 12.4 of the ACI 440.2R-17 design guidelines [11] establishes that the FRP pure axial tension strengthening is calculated using the shear provisions, which typically have short lengths, while the effective bond length is calculated using the flexural provisions. Thus, more research on thick and long ties is necessary to the debond force and deformation behavior can be characterized and the design guidelines updated.

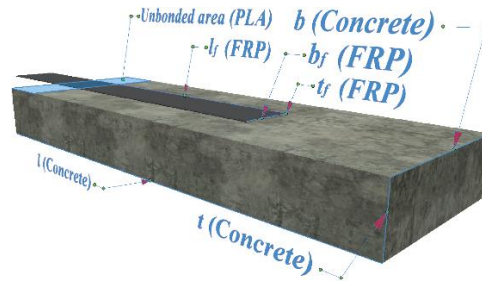


Fig. 1—Typical single-lap shear tests

A systematic literature review was conducted to collect and analyze all published research results from existing EB-FRP direct tension tests. Only the peak (debond) load has been used as a robust indicator of interfacial load-transfer performance due to the variability of the data published at different times, by different researchers and from different countries. Then, the behavior of thick and long FRP ties was investigated through a series of rigorous single lap shear tests. The experimental matrix extends the range of three critical parameters, concrete compressive strength, FRP thickness, and FRP bond length. The intention for this research is to fill the existing research gap in the realm of pure tension strengthening, specifically focusing on longer and thicker FRP ties more typically encountered in practical applications. Finally, the testing results and a proposed model are presented to discuss the design proposal for debonding strain with relation to the properties of concrete and FRP, specifically tailored for pure tension retrofitting applications.

SYSTEMATIC LITERATURE REVIEW

A systematic literature review was conducted using the Scopus and Web of Science databases spanning the period between 1994 and 2022. A thematic analysis based on the 2020 PRISMA Checklist [12] was employed to code and analyze the collected data, including research objectives, data acquisition systems, failure modes, and theoretical developments reported in the reviewed articles. Through the utilization of a meta-analysis, a more objective and robust outcome could be achieved compared to using potentially subjective and incomplete manual analysis methods. This methodology facilitated quantitative analysis, enabling the visualization of research trends through the generation of maps, and establishing connections between the research progress documented in the journal database and the relevant research topic.

A comprehensive overview of the procedures involved in this systematic literature review is included in Fig. 2, including the sorting of the database and the systematic assessment process. Initially, relevant topics were identified based on the research question, and papers were selected by applying six predefined criteria from two databases, Scopus and Web of Science, resulting in 38,793 and 36,056 journal papers respectively. The database underwent comprehensive screening and deduplication processes to ensure data integrity. During the screening phase, two authors of this paper acted as reviewers, using a three-step approach to evaluate titles and abstracts based on specific criteria as shown in the flowchart. The term 'combined' and 'deduplicated' refers to the process of integrating data from multiple sources to form a unified set of information and removal of duplicate entries or records from the database, respectively. Subsequently, a detailed review was conducted by two reviewers, who meticulously examined each paper to prevent any omissions or duplications. A structured database was established to facilitate this reviewing stage. Once all papers were thoroughly reviewed and the database was appropriately organized, a meticulous cleaning process was carried out. This process involved refining the database to enhance its reliability by excluding papers and variables that did not meet additional predefined criteria. For example, only test data obtained from single lap shear tests and under debonding failure modes were considered. Papers lacking

access to necessary data, such as material properties, were also excluded from the analysis. 88 journal articles and technical reports [4, 9, 10, 13-115] relevant to the topic and with robust and reliable data were compiled after the data were sorted and cleaned. Additionally, bibliometric analyses and the complexity of investigation (COI) evaluation system were utilized to provide both quantitative and qualitative perspectives [116]. The review highlighted the challenges and identified future research directions in the field, with a particular focus on the interfacial bond behavior of large-sized FRP ties strengthened in tension. An appendix with a comprehensive database with detailed information was provided. Readers interested can reach out to the authors to access the supplementary appendix, which are available on [Figshare](#).

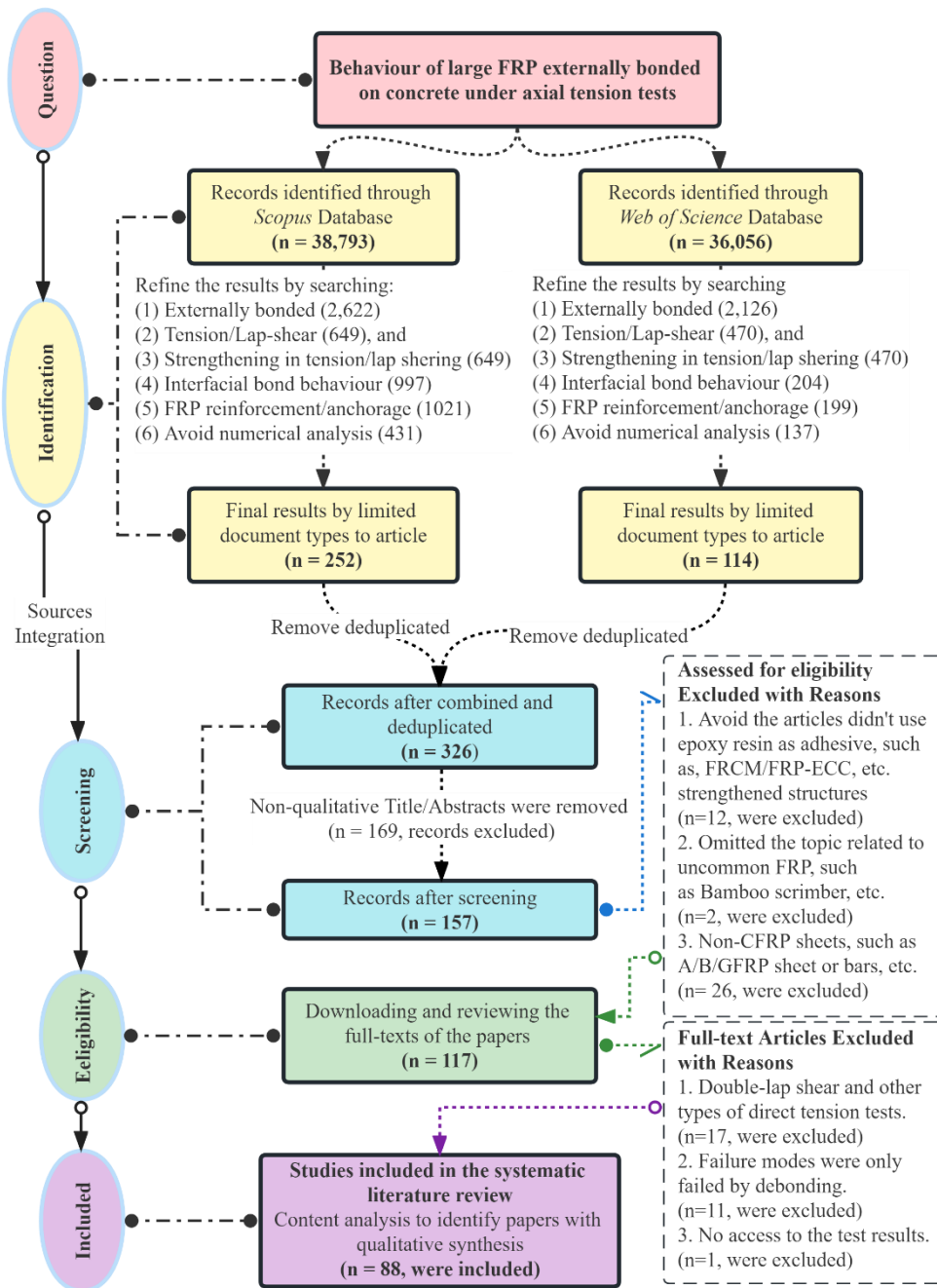


Fig. 2—The PRISMA flow diagram

A total of 1627 single lap shear tests on concrete members externally strengthened with FRP strips or ties were obtained. These tests encompassed the range of parameters described in Fig. 3, where the 4 quartiles, median, and outliers are reported. The outliers were calculated using the Tukey's fences method, which is based on the interquartile range (IQR). To begin, the first quartile (Q1) and the third quartile (Q3) of the dataset are determined. The IQR is then computed as the difference between Q3 and Q1. Next, the upper fence is calculated by adding 1.5 times the IQR to Q3, while the lower fence is obtained by subtracting 1.5 times the IQR from Q1. Any data points that fall above the upper fence or below the lower fence are considered outliers, as shown Fig. 3, where all outliers are marked outside the range defined by upper and lower fence.

Existing research predominantly focused on thin FRP ties with short bond lengths, while the distribution of concrete strength is quite robust. The importance of the ratio between stiffness of FRP ($nE_f t_f$) and concrete elastic modulus (E_c) is further discussed below.

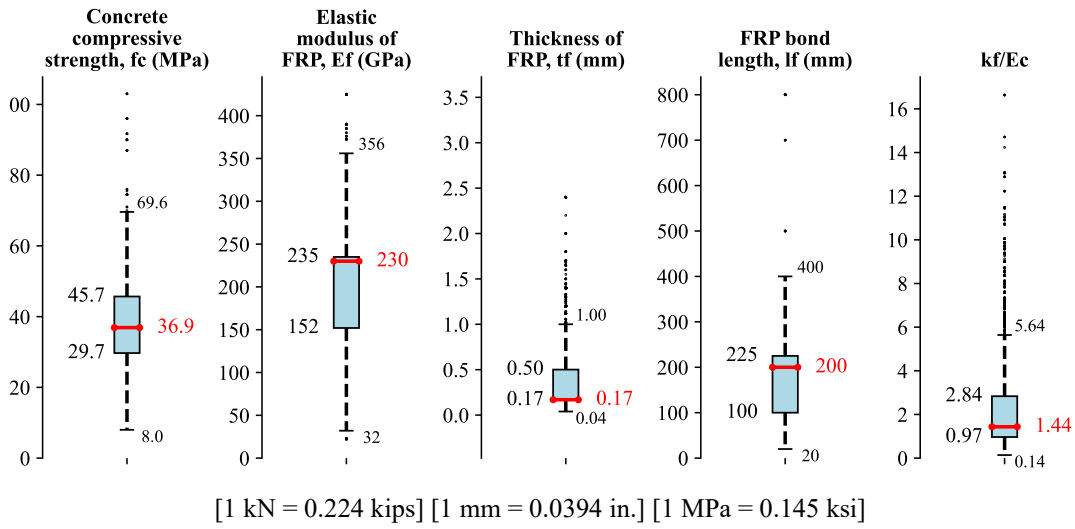


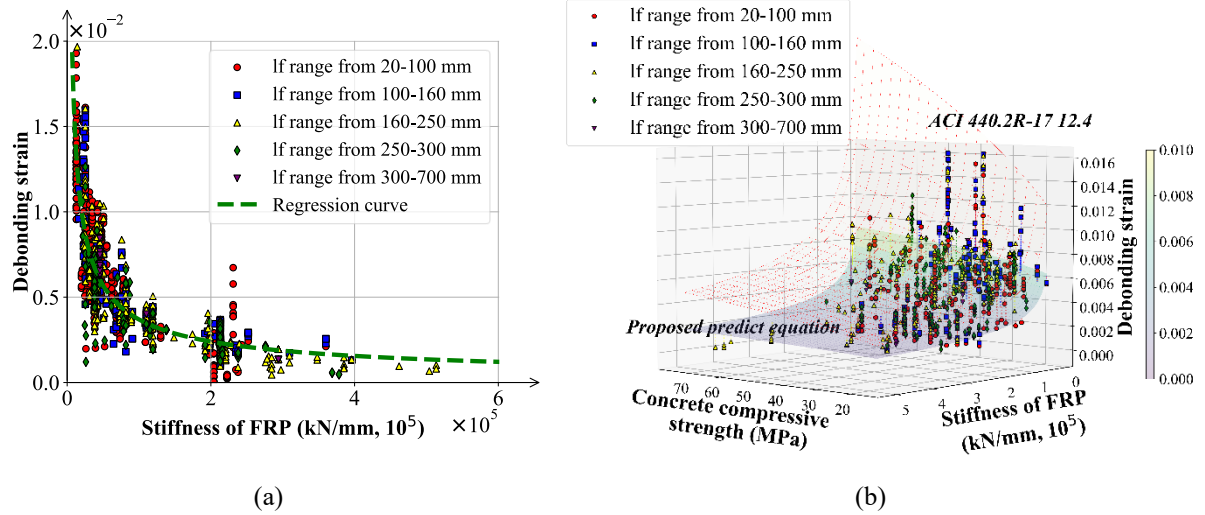
Fig. 3—Key parameters collected from published experimental works

A substantial data gap can be observed in the 2D and 3D scatter plot depicted in Fig. 4, indicating a lack of research on longer and stiffer (thicker) FRP. Therefore, future experimental studies should emphasize the behavior of larger-sized FRP on concrete structures. A 2D plot (Fig. 4a) with more distinct relationship between debonding strain and FRP stiffness, emphasizing the significant influence of FRP stiffness on system's load capacity. A 3D plot have also been plotted in Fig. 4b, The transparent red hatched surface corresponds to the equation derived from section 12.4 in ACI 440.2R-17 and shown in Eq. 1, which overpredicts the experimental strain values. Thus, further research is required to develop a predictive model for pure axial tension. In contrast, the colorful surface shown beneath the transparent red frame in Fig. 4b, which represents Eq. 2, adequately predicts the experimental strain. This equation is just an example, and a detailed version based on existing published data and recent experimental works is presented in following section.

$$\varepsilon_d = 0.75\varepsilon_u \quad \text{ACI 440.2R-17 Eq. (11.4.1.1)} \quad \text{Eq. 1}$$

$$\varepsilon_d = 4.764(k_f)^{-0.622} \quad \text{Regression algorithm as an example} \quad \text{Eq. 2}$$

Where ε_d is the debonding strain, ε_u is the strain at break, $k_f = nE_f t_f$ is stiffness of FRP, and $E_c \approx 4700\sqrt{f_c}$ concrete elastic modulus.



[1 kN = 0.224 kips] [1 mm = 0.0394 in.] [1 MPa = 0.145 ksi]

Fig. 4—2D and 3D scatter plots for all data collected

EXPERIMENTAL PROGRAM

Experimental testing was undertaken to evaluate the interfacial bond behavior of thick and long FRP ties bonded on concrete using the testing setup shown in Fig. 5(a). A load frame was used to secure the concrete blocks, while a servo-hydraulic actuator applied direct tension force to the FRP tie(s). A load cell was used to measure the applied loads, and three linear variable differential transformers (LVDTs) were used to measure the concrete block movement. LVDT-1 was positioned at the top, while LVDT-2 and LVDT-3 were positioned at 48 in. [1,219.2 mm] and 6 in. [152.4 mm] from the bottom of the block, respectively, to measure out of plane movement of the block. The displacement of the concrete block has been removed using LVDT-1, but the deformation of the gripping system, the unbonded length of FRP and of the testing machine itself has not been removed. A 3D optical deformation measurement digital image correlation (DIC) system was used to capture the displacements and strains on the surface of the FRP tie during the tests. The targets and ruler fixed to the concrete provide a means to verify the displacement of FRP ties during testing, as shown in Fig. 5(b), as well as serving as a reference and allow for calibration of the results in response to DIC analysis and concrete movements.

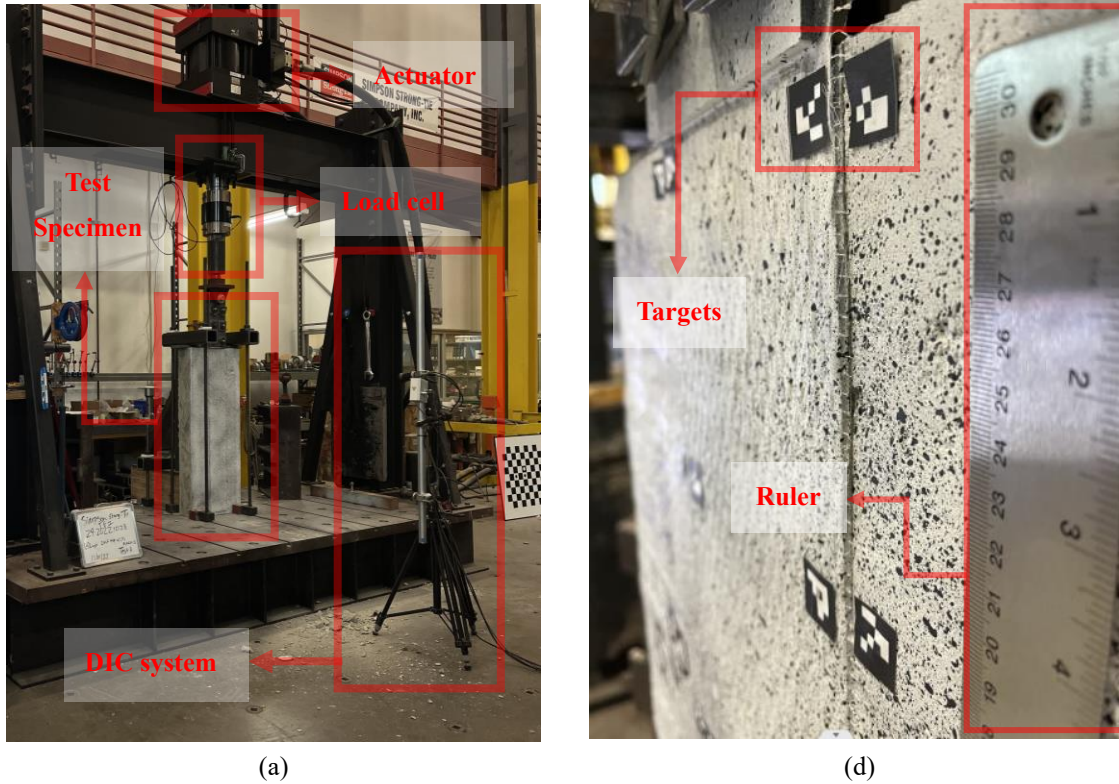
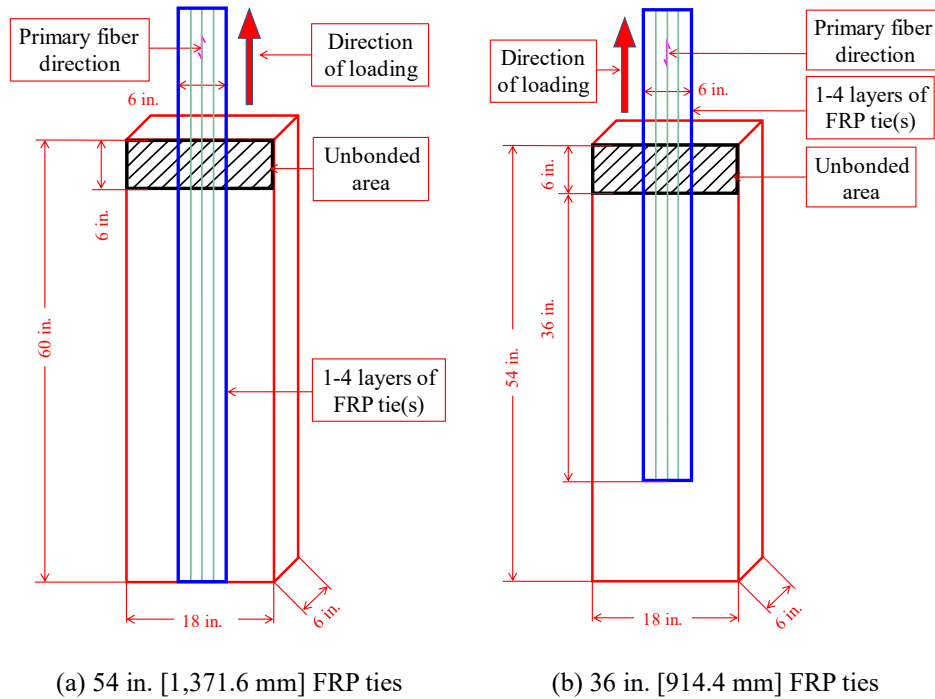


Fig. 5—Data acquisition systems: (a) Load cell and DIC system and (b) arrangement of targets and ruler

A total of 51 specimens were tested, consisting of 15 specimens tested during an initial campaign, and 36 follow-up specimens, all of them tested by Simpson Strong-Tie at the Tyrell Gilb Research Laboratory in Stockton, California. All concrete blocks had overall dimensions $6'' \times 18'' \times 54/60''$ [$152.4 \text{ mm} \times 457.2 \text{ mm} \times 1,371.6/1,524 \text{ mm}$] (depth \times width \times length) for recent/previous tests and were reinforced at their mid-depth with two and four #4 steel bars in the longitudinal and transverse directions, respectively. The typical specimens used in the testing are shown in Fig. 6(a) and (b). Concrete surfaces were prepared according to supplier and contractor specifications, aligned with best practice. Single-lap shear tests using static monotonic loading were used to characterize the behavior of the FRP-concrete interface.



(a) 54 in. [1,371.6 mm] FRP ties

(b) 36 in. [914.4 mm] FRP ties

Fig. 6—Typical configuration of specimens (a) previous tests, (b) in recent tests.

The previous tests investigated the influence of tie size and concrete compressive strength on the response of EB-FRP system, considering three critical parameters, being three levels of characteristic concrete compressive strength with 20.7 MPa [3,000 psi], 27.6 MPa [4,000 psi], and 41.4 MPa [6,000 psi], FRP thickness ranging from 1 mm [0.04 in.] to 6 mm [0.24 in.], and FRP bond lengths of 1,371.6 and 1,524 mm [54 and 60 in.]. The width of all FRP ties used in the specimens was 6 in. [152.4 mm], with an unbonded area of 6 in. [152.4 mm] to prevent damage to the concrete edges. A summary of the test matrix for the previous tested 15 specimens is provided in Table 1. Ties being 1 mm thick and installed on 20.7 MPa [3,000 psi] concrete, and 4 mm thick on 20.7 and 41.4 MPa [3,000 and 6,000 psi] were tested only once, the other test groups were repeated at least two times to improve the reliability of the results.

Table 1—Test matrix for 15 previous experimental works
 [1 kN = 0.224 kips] [1 mm = 0.0394 in.] [1 MPa = 0.145 ksi]

FRP stiffness ($k_f = E_f n t_f$)	FRP bond length (l_f)	
	60 in. (1,524 mm)	54 in. (1,371.6 mm)
FRP tie (370 g/m ² [11 oz./yd. ²]) with 2 layers ($t_f = 1$ mm)	20.7/41.4/41.4 MPa	N/A
FRP tie (1,490 g/m ² [44 oz./yd. ²]) with 1 layer ($t_f = 2$ mm)	20.7/20.7/20.7/41.4/41.4/41.4 MPa	27.6/27.6 MPa
FRP tie (740 g/m ² [22 oz./yd. ²]) with 4 layers ($t_f = 4$ mm)	N/A	20.7/41.4 MPa
FRP tie (1,490 g/m ² [44 oz./yd. ²]) with 3 layers ($t_f = 6$ mm)	N/A	27.6/27.6 MPa

Three critical parameters were considered to investigate the influence of tie size and concrete compressive strength on the EB-FRP tie response, being three levels of characteristic concrete compressive strength of 17.3 MPa [2,500 psi], 20.7 MPa [3,000 psi] and 34.5 MPa [5,000 psi]. The elastic modulus of the FRP used in this study is 98 GPa [14,200 ksi], FRP thickness with a range from one-layer (0.5 mm [0.02 in.]) to four layers (2 mm [0.08 in.]) of a typical weight of 370 g/m² [11 oz./yd.²], and FRP bond lengths of 304.8, 609.6 and 914.4 mm [12, 24 and 36 in.].

The width of FRP ties employed in all specimens was 152.4 mm [6 in.], with an unbonded area equal to 152.4 mm [6 in.] being applied to prevent breaking the edge of the concrete. A summary of the test matrix of the subsequent 36 specimens is included in Table 2. The values presented in each cell of the table represent the concrete compressive strengths utilized for the respective configurations. Only one repetition per permutation was tested, which is a significant limitation of the research project, but the study prioritized a comprehensive assessment of the strengthening performance across various FRP configurations rather than emphasizing statistical significance through multiple repetitions.

Table 2—Test matrix for 36 subsequent experimental works
[1 kN = 0.224 kips] [1 mm = 0.0394 in.] [1 MPa = 0.145 ksi]

$k_f = E_f n t_f$	l_f 12 in. (304.8 mm)	24 in. (609.6 mm)	36 in. (914.4 mm)
FRP tie with 1 layer ($t_f = 0.5$ mm)	19.2/19.5/36.1 MPa	19.2/19.5/36.1 MPa	19.2/19.5/36.1 MPa
FRP ties with 2 layers ($t_f = 1$ mm)	19.2/19.5/36.1 MPa	19.2/19.5/36.1 MPa	19.2/19.5/36.1 MPa
FRP ties with 3 layers ($t_f = 1.5$ mm)	19.2/19.5/36.1 MPa	19.2/19.5/36.1 MPa	19.2/19.5/36.1 MPa
FRP ties with 4 layers ($t_f = 2$ mm)	19.2/19.5/36.1 MPa	19.2/19.5/36.1 MPa	19.2/19.5/36.1 MPa

The compressive and splitting tensile strengths of the cylinders were 19.24 ± 1.32 MPa [$2,790.5 \pm 191.4$ psi], 19.53 ± 1.17 MPa [$2,832.6 \pm 169.7$ psi], and 36.14 ± 3.03 MPa [$5,241.7 \pm 49.3$ psi], and 3.99 ± 0.24 MPa [578.7 ± 34.8 psi] and 2.67 ± 0.34 MPa [387.3 ± 49.3 psi] respectively, tested in accordance with the ASTM C- 1140 and ASTM C496-1 standards. A total of 16 cylinders were tested for each of the three concrete mixes, with 8 cylinders subjected to compression testing and another 8 cylinders subjected to split tension testing. The mechanical properties of the FRP material were assessed through 42 coupon tests following the ASTM D3039 standard. The elastic modulus, tensile strength, and elongation at break of the FRP material were 105.4 ± 8.83 GPa [$1,5287 \pm 1,280.7$ ksi], $1,363.5 \pm 136.9$ MPa [197.8 ± 19.9 ksi], and $1.39 \pm 0.17\%$, respectively. Detailed data on the mechanical properties of the materials can be found in the appendix.

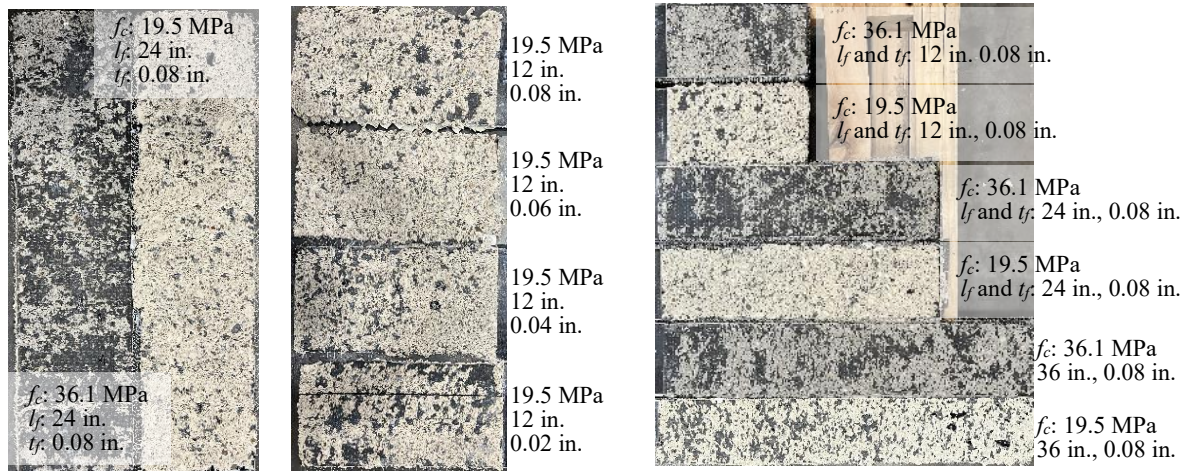
RESULTS AND DISCUSSION

The complete dataset including the 1627 published data, the 15 previous tests and the 36 tests is included in tables in Appendix, but the detailed results are not presented in this section due to space limitations. The subsequent subsections explore the failure modes observed, impact of the key variables mentioned earlier, as well as the interplay between three critical attributes and the capacity for FRP debonding.

Failure modes

The failure mode observed in all the specimens was interfacial bond failure as depicted in Fig. 7, resulting in the release of significant fracture energy, but with differences depending on the concrete strength and tie stiffness. The FRP tie tested on high strength concrete (Fig. 7a left) had significantly less concrete material still attached to the FRP than those tested on lower strength concrete (Fig. 7a right), corroborating the hypothesis that the failure mode and therefore capacity depends on the tensile strength of the concrete. The use of thicker ties also led to increased concrete peeling when debonding occurred (Fig. 7b from bottom to top). Combined with the relationship between concrete compressive strength (f_c) and its elastic modulus ($E_c \approx 4700\sqrt{f_c}$). These two observations led us to hypothesize that the debond behavior and capacity is related to a combination of both the stiffness of the

FRP (nE_ft_f) and the concrete elastic modulus (E_c). Premature debond failure due to installation errors were excluded and are marked with red stars in Fig. 8(c), (d), and (g). These failures highlight the importance of adequate installation when working with FRP materials [117].



(a) higher to lower

(b) thick to thin

(c) long to short

[1 mm = 0.0394 in.] [1 MPa = 0.145 ksi = 145 psi]

Fig. 7— Comparison of fractured surfaces of FRP ties considering:
(a) concrete strength, (b) thickness of FRP, and (c) bond lengths of FRP.

Load-displacement response

The load-slip response of recent 36 tests and previous 15 tests are presented in Fig. 8(a) to (i) and (j) to (l), respectively. Each test in the figure is represented by three numbers, indicating the concrete compressive strength, the bond length of the FRP, and the number of its layers, respectively. Thicker and consequently stiffer FRP tie configurations exhibited a higher strength capacity, but the effect of concrete strength on FRP tie response and debond capacity is less significant. All tested bond lengths exhibited a bilinear response, with an initial elastic phase and a certain level of post-debond deformation capacity, which was influenced by the bond length, concrete compressive strength, and FRP stiffness. The significant increase in post-debond deformation capacity observed with longer FRP bond lengths is noteworthy, as shown in Fig. 8(f) and (i). The deformation almost doubled when a 36 in. [914.4 mm] bond length was adopted compared to a 12 in. [304.8 mm] bond length. This deformation capacity is also dependent on the stiffness of the FRP. For instance, a one-layer thick tie exhibited a greater deformation capacity compared to the four-layer thick ties despite having the same bond length. The system capacity displayed limited sensitivity to variations in concrete compressive strength, irrespective of the bond length or stiffness of the FRP ties, as evidenced by Fig. 8(b) and (h).

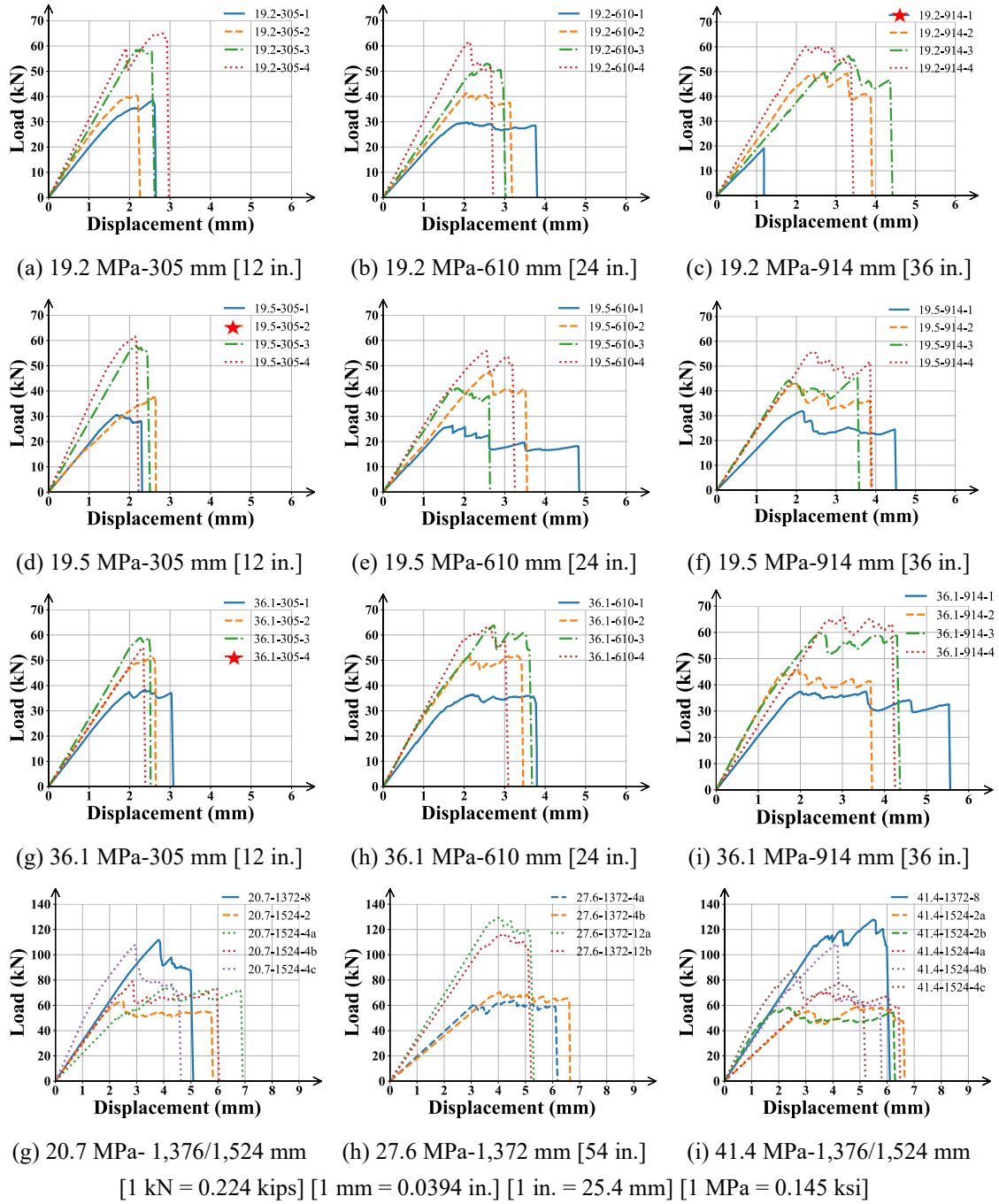
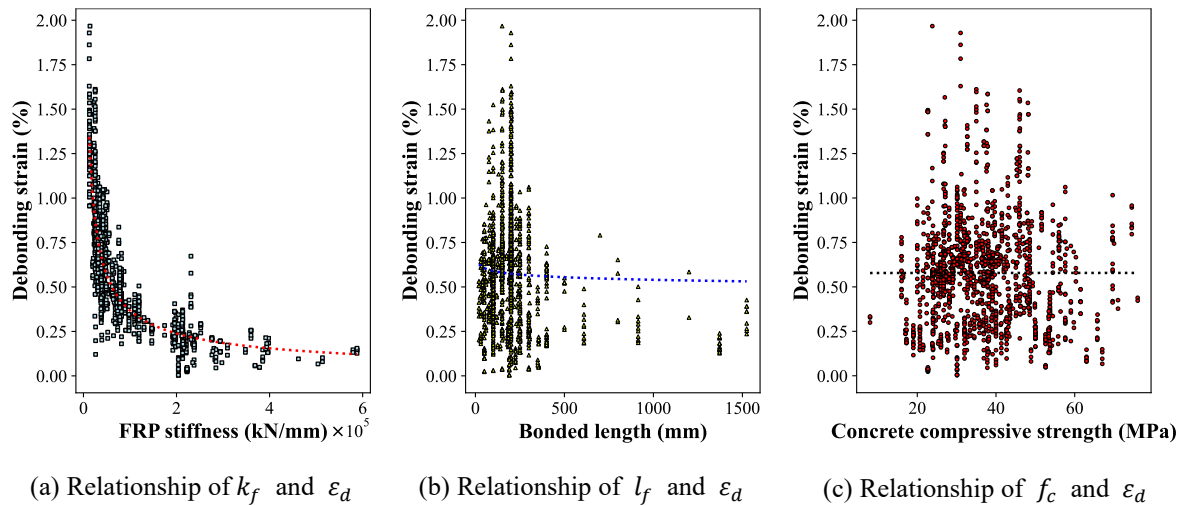


Fig. 8—Load-Displacement response

Acknowledging the limitations of the experimental work is important. This study involved only one single test per specimen without any replications, which may impact the assessment of the findings. Additionally, the force-displacement measurements were captured using a load cell, and while the displacement of the concrete block has been removed using LVDT-1, the deformation of the gripping system and of the testing machine itself was not taken into account. To address this issue, and to fully understand the deformation response of the ties, ongoing analysis using Digital Image Correlation (DIC) is being completed, which is a method gaining more traction in the field of FRP [118]. The results reported herein being focused on debond force to address critical shortcomings in design guidelines.

Parametric analysis

The distribution of three critical parameters including previously published and recently obtained data related to debonding capacity is illustrated in Fig. 9. These parameters include the FRP stiffness (k_f), bond length (l_f), and concrete compressive strength (f_c). The dashed trendlines in the scatter plots, generated using a second-order regression algorithm, highlight the overall trends among the parameters but cannot be used to making predictions or calculations. The trendlines clearly demonstrate that debonding strain is primarily influenced by k_f , and bond length (Fig. 9a and b), with k_f exhibiting a steeper trendline. The relationship between compressive strength and debonding strain shown in Fig. 9c is not as apparent as for bond length (Fig. 9b) and FRP stiffness (Fig. 9a). The main reason is that the compressive strength is not related to the failure mechanism, but rather the stiffness or modulus of elasticity is the key concrete property that influences failure. In other words, the stress (strength) at which the concrete fails are not the critical parameter, the elastic response to the concrete being loaded is the critical parameter. However, the two of them are linear related ($E_c \approx 4700\sqrt{f_c}$) and compressive strength is the most commonly used parameter both in research and in practical design. Additionally, the compressive strength is assessed in Fig. 9c in isolation, i.e. not in combination with or in relation to any other factor. When the concrete strength (or rather the modulus of elasticity) is assessed in combination with the FRP stiffness the impact on debond strain becomes apparent.



[1 kN = 0.224 kips] [1 mm = 0.0394 in.] [1 MPa = 0.145 ksi]

Fig. 9—Relationship between debonding strain and critical variables considered

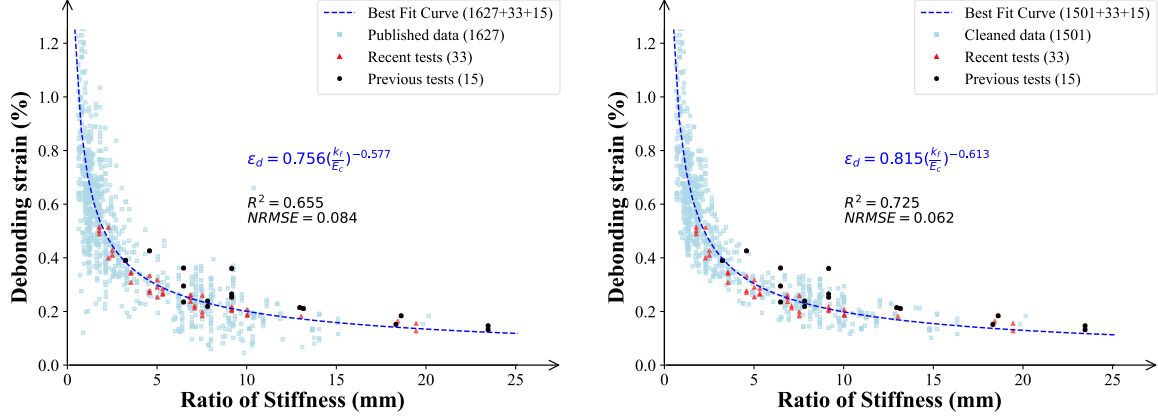
(Dataset includes 1,627 published data, 15 previous test, and 33 recent tests)

DESIGN MODEL PROPOSAL

The proposed design model is based on the empirical observations from the failure modes shown in Fig. 7 and force-displacement curves (Fig. 8). The analysis shown in Fig 9 indicates that concrete compressive strength (f_c) has a certain effect on debond strain, and the influence of FRP tie length (l_f) on debond strain behavior is found to be negligible. Conversely, the stiffness of FRP emerges as the predominant factor influencing debond strain, but with a moderate influence of concrete strength (f_c). Therefore, the ratio of stiffness of FRP and concrete elastic modulus is used as a predictor of debond strain. A regression analysis using a power equation was conducted to statistically analyze the data, forming the basis for the design model, as plotted in Fig. 10. The objective of this model is to accurately predict the debond strain based on the stiffness ratio k_f/E_c .

The presence of scattered dots around the equation in Fig. 10a is the result of the original published data potentially having relatively low quality. These noise dots are outliers that lie outside the reliable range of the data, as

determined through the Tukey's Fence method outlined above, which is shown in the box and whiskers plots from Fig. 3. A data refinement process was conducted to improve the data quality and mitigate the impact of outliers. As a result, a refined equation was obtained, as depicted in Fig. 10b, which exhibited an enhanced R^2 (Goodness of fit) value of 0.725 and a decreased NRMSE (Normalized Root Mean Square Error) of 0.062.



(a) Proposed equation

(b) After noise cleaning

[1 kN = 0.224 kips] [1 mm = 0.0394 in.]

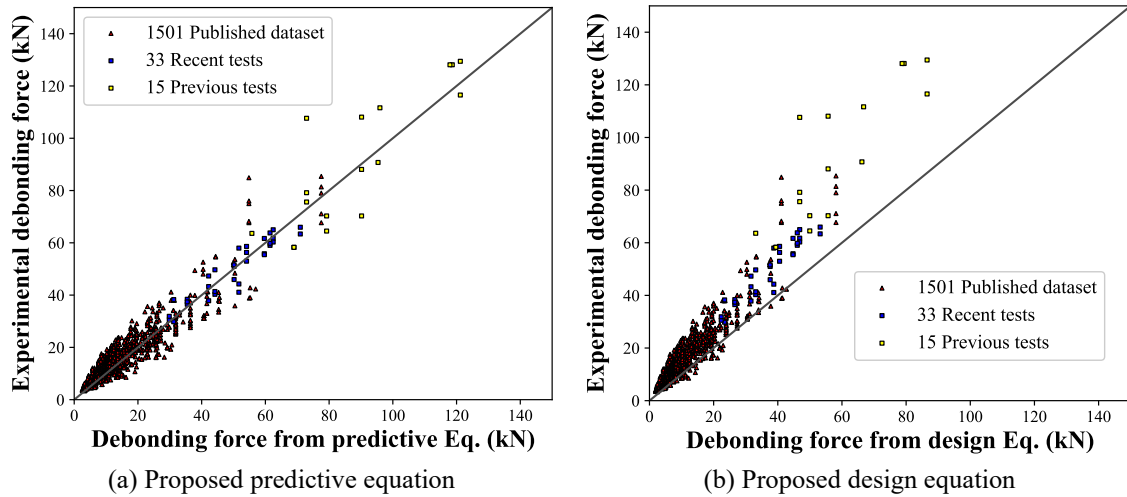
Fig. 10—Proposed equation for all data

The proposed equation for predicting debonding force, denoted as Eq. 3, is a reformatting of the equation from the equation shown in Fig. 10b. To determine the optimal coefficient, an iterative analysis was performed by comparing the expected debond strain with the actual data. This iterative process ensures that a minimum of 95% of the data points lie above the 1:1 line, demonstrating a strong alignment between the calculated values and the experimental data. The resulting design equation, Eq. 4, reflects this approach and is supported by the characteristic test data consistently falling above the 1:1 line.

$$\varepsilon_d = 45.22 \sqrt{\frac{\sqrt{f'_c}}{nt_f E_f}} \quad (\%) \quad \text{(Predictive equation)} \quad \text{Eq. 3}$$

$$\varepsilon_d = 33.64 \sqrt{\frac{\sqrt{f'_c}}{nt_f E_f}} \leq 0.75 \varepsilon_u \quad (\%) \quad \text{(Design Equation)} \quad \text{Eq. 4}$$

A comparison between the experimental debonding force and the predicted/design values based on the proposed provisions (Eq. 3 and Eq. 4) are depicted in Fig. 11 (a) and (b), respectively. The plots shows that the predict values have a good correlation with the experimental values, and that the design values maintain a safe range. A comparison between the experimental data and the more commonly used design guidelines [11, 119, 120] was previously compiled [9], which shows that these documents cannot accurately capture the behaviour of long ties.



[1 kN = 0.224 kips] [1 mm = 0.0394 in.]

Fig. 11—Q-Q plot for proposed equations

CONCLUSION AND RECOMMENDATIONS

This study conducted a systematic literature review to collect published data on FRP ties on pure tension configuration, resulting in a database of 1627 data points from 88 publications. The literature review highlighted the lack of data on long and thick FRP ties, but the investigation of concrete strength was robust. Therefore, various configurations of FRP ties (thicker and longer) were experimentally investigated with different concrete strengths. The new experimental data was analyzed from a force perspective, leaving the deformation response out of this manuscript due to a lack of space and for future publication. Then, all the collected data (1627 from published research, 51 from the new experimental work) was studied holistically, providing key insights into the critical parameters that affect debond strain. Finally, we proposed a design equation to address the inclusion of thicker and longer FRP ties in EB-FRP systems for pure tension strengthening. The main conclusions are as follows.

- All specimens exhibited debonding failure, with thicker FRP ties influencing load-bearing capacity and longer ties showing greater post-debond deformation capacity.
- The debonding load capacity showed a certain correlation with concrete strength, but limited sensitivity to changes in bond length.
- Debond strain correlates non-linearly with FRP-to-concrete stiffness ratio, following a power relationship.
- The proposed equation predicts debonding loads reasonably accurate, considering properties of concrete and FRP.

ACKNOWLEDGMENTS

The author appreciates the financial support from the MBIE Smart Ideas (Endeavour Fund). Simpson Strong-Tie Inc. providing materials and research facilities is also gratefully acknowledged.

REFERENCES

- [1] Attari, N., S. Amziane, and M. Chemrouk, *Flexural strengthening of concrete beams using CFRP, GFRP and hybrid FRP sheets*. Construction and Building Materials, 2012. **37**: p. 746-757.
- [2] Sun, W., J.O. Jirsa, and W.M. Ghannoum, *Behavior of Anchored Carbon Fiber-Reinforced Polymer Strips Used for Strengthening Concrete Structures*. ACI Materials Journal, 2016. **113**(2).
- [3] Triantafillou, T.C., *Shear strengthening of reinforced concrete beams using epoxy-bonded FRP composites*.

ACI structural journal, 1998. **95**: p. 107-115.

[4] Xiong, G., et al., *A way for preventing tension delamination of concrete cover in midspan of FRP strengthened beams*. Construction and Building Materials, 2007. **21**(2): p. 402-408.

[5] Liu, S., et al., *Debonding detection and monitoring for CFRP reinforced concrete beams using piezoceramic sensors*. Materials, 2019. **12**(13): p. 2150.

[6] Täljsten, B., *Strengthening of beams by plate bonding*. Journal of materials in civil engineering, 1997. **9**(4): p. 206-212.

[7] del Rey Castillo, E., M. Griffith, and J. Ingham, *Seismic behavior of RC columns flexurally strengthened with FRP sheets and FRP anchors*. Composite Structures, 2018. **203**: p. 382-395.

[8] Hamilton Iii, H. and C. Dolan, *Flexural capacity of glass FRP strengthened concrete masonry walls*. Journal of Composites for Construction, 2001. **5**(3): p. 170-178.

[9] del Rey Castillo, E., et al., *FRP Tension Ties: State-of-the-Art Review of Existing Design Guidance for Debonding Capacity and Applicability to Concrete Diaphragm Seismic Strengthening*. Journal of Composites for Construction, 2022. **26**(2): p. 04022014.

[10] Ormeno, M., et al. *Capacity of diaphragm strengthened with FRP: Comparison between ACI 440.2 R and in-situ tests*. in *Proceedings of the 2019 Pacific Conference on Earthquake Engineering (NZSEE/PCEE)*, SkyCity, AK, New Zealand. 2019.

[11] 440.2R, A., *ACI 440. 2R-17 Guide for the Design and Construction of Externally Bonded FRP Systems for Strengthening Concrete Structures*. 2017: American Concrete Institute.

[12] Page, M.J., et al., *The PRISMA 2020 statement: an updated guideline for reporting systematic reviews*. International journal of surgery, 2021. **88**: p. 105906.

[13] Lam, L. and J.G. Teng, *Design-oriented stress-strain model for FRP-confined concrete*. Construction and building materials, 2003. **17**(6-7): p. 471-489.

[14] Täljsten, B., *Plate bonding: Strengthening of existing concrete structures with epoxy bonded plates of steel or fibre reinforced plastics*. 1994, Luleå tekniska universitet.

[15] Chajes, M.J., W.W. Finch, and T.A. Thomson, *Bond and force transfer of composite-material plates bonded to concrete*. Structural Journal, 1996. **93**(2): p. 209-217.

[16] Seracino, R., M. Raizal Saifulnaz, and D. Oehlers, *Generic debonding resistance of EB and NSM plate-to-concrete joints*. Journal of Composites for Construction, 2007. **11**(1): p. 62-70.

[17] Carloni, C. and K.V. Subramaniam, *Investigation of sub-critical fatigue crack growth in FRP/concrete cohesive interface using digital image analysis*. Composites Part B: Engineering, 2013. **51**: p. 35-43.

[18] Ghahsareh, F.M. and D. Mostofinejad, *Effects of groove angle and pattern on cfrp-to-concrete bond behavior of ebrog joints: Comparison of diagonal with longitudinal and transverse grooves*. Construction and Building Materials, 2022. **342**: p. 127980.

[19] Ghaleh, R.Z. and D. Mostofinejad, *Behaviour of EBRIG CFRP sheet-concrete joint: Comparative assessment with EBR and EBROG methods*. Construction and Building Materials, 2022. **346**: p. 128374.

[20] Moshiri, N., et al., *Bond resistance of prestressed CFRP strips attached to concrete by using EBR and EBROG strengthening methods*. Construction and Building Materials, 2021. **266**: p. 121209.

[21] Yuan, C., et al., *Interfacial bond behaviour between hybrid carbon/basalt fibre composites and concrete under dynamic loading*. International Journal of Adhesion and Adhesives, 2020. **99**: p. 102569.

[22] Al-Lami, K., P. Colombi, and T. D'Antino, *Influence of hygrothermal ageing on the mechanical properties of CFRP-concrete joints and of their components*. Composite Structures, 2020. **238**: p. 111947.

[23] Mofrad, M.H., D. Mostofinejad, and A. Hosseini, *A generic non-linear bond-slip model for CFRP composites bonded to concrete substrate using EBR and EBROG techniques*. Composite Structures, 2019. **220**: p. 31-44.

- [24] Pan, Y. and G. Xian, *Influence of long-term outdoor exposure in a frigid zone on the CFRP-to-concrete bond behavior*. Construction and Building Materials, 2019. **215**: p. 462-474.
- [25] Ghorbani, M., D. Mostofinejad, and A. Hosseini, *Experimental investigation into bond behavior of FRP-to-concrete under mixed-mode I/II loading*. Construction and Building Materials, 2017. **132**: p. 303-312.
- [26] Ferrier, E., O. Rabinovitch, and L. Michel, *Mechanical behavior of concrete–resin/adhesive–FRP structural assemblies under low and high temperatures*. Construction and Building Materials, 2016. **127**: p. 1017-1028.
- [27] Biscaia, H.C., M.A. Silva, and C. Chastre, *Factors influencing the performance of externally bonded reinforcement systems of GFRP-to-concrete interfaces*. Materials and Structures, 2015. **48**: p. 2961-2981.
- [28] Zhang, W. and J.-B. Yan, *Fatigue properties of shear–peeling debonding between CFRP plates and concrete*. Magazine of Concrete Research, 2016. **68**(23): p. 1210-1224.
- [29] Firmo, J., et al., *Experimental characterization of the bond between externally bonded reinforcement (EBR) CFRP strips and concrete at elevated temperatures*. Cement and Concrete Composites, 2015. **60**: p. 44-54.
- [30] Shen, D., et al., *Dynamic bond stress-slip relationship between basalt FRP sheet and concrete under initial static loading*. Journal of Composites for Construction, 2015. **19**(6): p. 04015012.
- [31] Gravina, R., S.A. Hadigheh, and S. Setunge, *Interfacial bond strength of resin-impregnated fibre-reinforced polymer laminates bonded to concrete using vacuum and heat: Experimental study*. Australian Journal of Structural Engineering, 2014. **15**(2): p. 189-201.
- [32] Quiertant, M., et al., *Effects of ageing on the bond properties of carbon fiber reinforced polymer/concrete adhesive joints: investigation using a modified double shear test*. Journal of Testing and Evaluation, 2017. **45**(6).
- [33] Michels, J., et al., *Anchorage resistance of CFRP strips externally bonded to various cementitious substrates*. Composites Part B: Engineering, 2014. **63**: p. 50-60.
- [34] Hosseini, A. and D. Mostofinejad, *Effective bond length of FRP-to-concrete adhesively-bonded joints: Experimental evaluation of existing models*. International Journal of Adhesion and Adhesives, 2014. **48**: p. 150-158.
- [35] Yang, G., et al., *Uniaxial tensile stress-strain relationships of RC elements strengthened with FRP sheets*. Journal of Composites for Construction, 2016. **20**(3): p. 04015075.
- [36] Mostofinejad, D., K. Sanginabadi, and M.R. Eftekhari, *Effects of coarse aggregate volume on CFRP-concrete bond strength and behavior*. Construction and Building Materials, 2019. **198**: p. 42-57.
- [37] Hallonet, A., L. Michel, and E. Ferrier, *Investigation of the bond behavior of flax FRP strengthened RC structures through double lap shear testing*. Composites Part B: Engineering, 2016. **100**: p. 247-256.
- [38] Zhang, W., *Experimental study on shear-peeling bond strength between a CFRP plate and concrete*. Magazine of Concrete Research, 2016. **68**(11): p. 568-580.
- [39] Zhang, W., *Experimental study on fatigue behaviour of CFRP plates externally bonded to concrete substrate*. Structural Concrete, 2016. **17**(2): p. 235-244.
- [40] Shi, J.-W., W.-H. Cao, and Z.-S. Wu, *Effect of adhesive properties on the bond behaviour of externally bonded FRP-to-concrete joints*. Composites Part B: Engineering, 2019. **177**: p. 107365.
- [41] Zhu, H., et al., *Digital image correlation measurement of the bond–slip relationship between fiber-reinforced polymer sheets and concrete substrate*. Journal of Reinforced Plastics and Composites, 2014. **33**(17): p. 1590-1603.
- [42] Mensah, C., A.O. Bonsu, and Z. Wang, *Interfacial behavior of externally bonded BFRP-to-concrete joints using different epoxy adhesives*. International Journal of Adhesion and Adhesives, 2022. **119**: p. 103277.
- [43] Zhang, P., et al. *Influence factors analysis of the interfacial bond behavior between GFRP plates, concrete*. in Structures. 2020. Elsevier.
- [44] Yuan, C., et al., *Effect of aggregate size on bond behaviour between basalt fibre reinforced polymer sheets*

and concrete. Composites Part B: Engineering, 2019. **158**: p. 459-474.

[45] Fazli, H., et al., *Influence of coarse aggregate size on the bonding between CFRP Sheets and metakaolin-based geopolymer concrete and ordinary concrete*. Journal of Composites for Construction, 2022. **26**(2): p. 04022004.

[46] Sanginabadi, K. and D. Mostofinejad, *Effect of aggregate content on the CFRP-concrete effective bond length: An experimental and analytical study*. Composite Structures, 2021. **269**: p. 114044.

[47] Tajmir-Riahi, A., N. Moshiri, and D. Mostofinejad, *Bond mechanism of EBROG method using a single groove to attach CFRP sheets on concrete*. Construction and Building Materials, 2019. **197**: p. 693-704.

[48] Yuan, C., et al., *Bond behavior between basalt fibres reinforced polymer sheets and steel fibres reinforced concrete*. Engineering Structures, 2018. **176**: p. 812-824.

[49] Soares, S., et al., *Influence of surface preparation method on the bond behavior of externally bonded CFRP reinforcements in concrete*. Materials, 2019. **12**(3): p. 414.

[50] Zhang, Z., et al., *Experimental Investigation on the Interfacial Debonding between FRP Sheet and Concrete under Medium Strain Rate*. International Journal of Polymer Science, 2019. **2019**: p. 1-13.

[51] Salimian, M.S. and D. Mostofinejad, *Experimental evaluation of CFRP-concrete bond behavior under high loading rates using particle image velocimetry method*. Journal of Composites for Construction, 2019. **23**(3): p. 04019010.

[52] Moghaddas, A., D. Mostofinejad, and E. Ilia, *Empirical FRP-concrete effective bond length model for externally bonded reinforcement on the grooves*. Composites Part B: Engineering, 2019. **172**: p. 323-338.

[53] Moshiri, N., et al., *Experimental and analytical study on CFRP strips-to-concrete bonded joints using EBROG method*. Composites Part B: Engineering, 2019. **158**: p. 437-447.

[54] Moghaddas, A. and D. Mostofinejad, *Empirical FRP-concrete bond strength model for externally bonded reinforcement on grooves*. Journal of Composites for Construction, 2019. **23**(2): p. 04018080.

[55] Yuan, C., et al., *Strain rate effect on interfacial bond behaviour between BFRP sheets and steel fibre reinforced concrete*. Composites Part B: Engineering, 2019. **174**: p. 107032.

[56] Tajmir-Riahi, A., N. Moshiri, and D. Mostofinejad, *Inquiry into bond behavior of CFRP sheets to concrete exposed to elevated temperatures–Experimental & analytical evaluation*. Composites Part B: Engineering, 2019. **173**: p. 106897.

[57] Yuan, C., et al., *Influence of concrete strength on dynamic interfacial fracture behaviour between fibre reinforced polymer sheets and concrete*. Engineering Fracture Mechanics, 2020. **229**: p. 106934.

[58] Mostofinejad, D., et al., *Investigating the effects of concrete compressive strength, CFRP thickness and groove depth on CFRP-concrete bond strength of EBROG joints*. Construction and Building Materials, 2018. **189**: p. 323-337.

[59] Yuan, C., et al., *Dynamic interfacial bond behaviour between basalt fiber reinforced polymer sheets and concrete*. International Journal of Solids and Structures, 2020. **202**: p. 587-604.

[60] Carlos, T.B. and J.P.C. Rodrigues, *Experimental bond behaviour of a CFRP strengthening system for concrete elements at elevated temperatures*. Construction and Building Materials, 2018. **193**: p. 395-404.

[61] Ghorbani, M., D. Mostofinejad, and A. Hosseini, *Bond behavior of CFRP sheets attached to concrete through EBR and EBROG joints subject to mixed-mode I/II loading*. Journal of Composites for Construction, 2017. **21**(5): p. 04017034.

[62] Al-Tamimi, A.K., et al., *Durability of the bond between CFRP plates and concrete exposed to harsh environments*. Journal of Materials in Civil Engineering, 2015. **27**(9): p. 04014252.

[63] Yuan, C., et al., *Bond behaviour between hybrid fiber reinforced polymer sheets and concrete*. Construction and Building Materials, 2019. **210**: p. 93-110.

- [64] Santandrea, M., I.A.O. Imohamed, and C. Carloni, *Width effect in FRP–concrete debonding mechanism: A new formula*. Journal of Composites for Construction, 2020. **24**(4): p. 04020024.
- [65] Ueno, S., H. Toutanji, and R. Vuddandam, *Introduction of a stress state criterion to predict bond strength between FRP and concrete substrate*. Journal of Composites for Construction, 2015. **19**(1): p. 04014024.
- [66] Ko, H., et al., *Development of a simplified bond stress–slip model for bonded FRP–concrete interfaces*. Construction and Building Materials, 2014. **68**: p. 142-157.
- [67] Wu, Y.-F. and C. Jiang, *Quantification of bond-slip relationship for externally bonded FRP-to-concrete joints*. Journal of Composites for Construction, 2013. **17**(5): p. 673-686.
- [68] Zhang, H. and S.T. Smith, *Fibre-reinforced polymer (FRP)-to-concrete joints anchored with FRP anchors: tests and experimental trends*. Canadian Journal of Civil Engineering, 2013. **40**(11): p. 1103-1116.
- [69] Hosseini, A. and D. Mostofinejad, *Experimental investigation into bond behavior of CFRP sheets attached to concrete using EBR and EBROG techniques*. Composites Part B: Engineering, 2013. **51**: p. 130-139.
- [70] Ohu, R., et al., *Effect of surface treatment on bond of embedded carbon fiber-reinforced polymer plates*. Journal of composite materials, 2013. **47**(24): p. 3065-3079.
- [71] Toutanji, H., M. Han, and E. Ghorbel, *Interfacial bond strength characteristics of FRP and RC substrate*. Journal of Composites for Construction, 2012. **16**(1): p. 35-46.
- [72] Alam, M.S., T. Kanakubo, and A. Yasojima, *Shear-Peeling Bond Strength between Continuous Fiber Sheet and Concrete*. ACI Structural Journal, 2012. **109**(1).
- [73] Carloni, C., et al., *Experimental determination of FRP–concrete cohesive interface properties under fatigue loading*. Composite Structures, 2012. **94**(4): p. 1288-1296.
- [74] Bilotta, A., et al., *Bond efficiency of EBR and NSM FRP systems for strengthening concrete members*. Journal of Composites for Construction, 2011. **15**(5): p. 757-772.
- [75] Bilotta, A., M. Di Ludovico, and E. Nigro, *FRP-to-concrete interface debonding: Experimental calibration of a capacity model*. Composites Part B: Engineering, 2011. **42**(6): p. 1539-1553.
- [76] Woo, S.-K. and Y. Lee, *Experimental study on interfacial behavior of CFRP-bonded concrete*. KSCE Journal of Civil Engineering, 2010. **14**: p. 385-393.
- [77] Czaderski, C., K. Soudki, and M. Motavalli, *Front and side view image correlation measurements on FRP to concrete pull-off bond tests*. Journal of Composites for Construction, 2010. **14**(4): p. 451-463.
- [78] Carloni, C. and K.V. Subramaniam, *Direct determination of cohesive stress transfer during debonding of FRP from concrete*. Composite Structures, 2010. **93**(1): p. 184-192.
- [79] Zhou, Y., *Analytical and experimental study on the strength and ductility of FRP-reinforced high strength concrete beam*. Chinese.] Ph. D. Dissertation, Dalian Univ. of Technology, 2009.
- [80] Fen, Z., et al., *Experimental study on bond behavior between carbon fiber reinforced polymer and concrete*. Struct. Eng, 2008. **24**(4): p. 154-163.
- [81] Pellegrino, C., D. Tinazzi, and C. Modena, *Experimental study on bond behavior between concrete and FRP reinforcement*. Journal of Composites for Construction, 2008. **12**(2): p. 180-189.
- [82] Pham, H.B. and R. Al-Mahaidi, *Modelling of CFRP-concrete shear-lap tests*. Construction and Building Materials, 2007. **21**(4): p. 727-735.
- [83] Toutanji, H., et al., *Prediction of interfacial bond failure of FRP–concrete surface*. Journal of composites for construction, 2007. **11**(4): p. 427-436.
- [84] Ko, H. and Y. Sato, *Bond stress–slip relationship between FRP sheet and concrete under cyclic load*. Journal of Composites for Construction, 2007. **11**(4): p. 419-426.
- [85] Cao, S., et al., *ESPI measurement of bond-slip relationships of FRP-concrete interface*. Journal of composites for construction, 2007. **11**(2): p. 149-160.

- [86] Subramaniam, K.V., C. Carloni, and L. Nobile, *Width effect in the interface fracture during shear debonding of FRP sheets from concrete*. Engineering Fracture Mechanics, 2007. **74**(4): p. 578-594.
- [87] Ali-Ahmad, M., K. Subramaniam, and M. Ghosn, *Experimental investigation and fracture analysis of debonding between concrete and FRP sheets*. Journal of engineering mechanics, 2006. **132**(9): p. 914-923.
- [88] Ferracuti, B., *Strengthening of RC structures by FRP: Experimental analyses and numerical modelling*. University of Bologna, Bologna, 2006.
- [89] Lu, X., et al., *Bond-slip models for FRP sheets/plates bonded to concrete*. Engineering structures, 2005. **27**(6): p. 920-937.
- [90] Yao, J., J. Teng, and J.F. Chen, *Experimental study on FRP-to-concrete bonded joints*. Composites Part B: Engineering, 2005. **36**(2): p. 99-113.
- [91] Ali-Ahmad, M., *Debonding of FRP from concrete in strengthening applications: experimental investigation and theoretical validation*. 2005: City University of New York.
- [92] Lu, X., et al., *Meso-scale finite element model for FRP sheets/plates bonded to concrete*. Engineering structures, 2005. **27**(4): p. 564-575.
- [93] Dai, J., T. Ueda, and Y. Sato, *Development of the nonlinear bond stress-slip model of fiber reinforced plastics sheet-concrete interfaces with a simple method*. Journal of composites for construction, 2005. **9**(1): p. 52-62.
- [94] Zhou, Y., et al., *Explicit neural network model for predicting FRP-concrete interfacial bond strength based on a large database*. Composite Structures, 2020. **240**: p. 111998.
- [95] Yao, J., *Debonding failures in RC beams and slabs strengthened with FRP plates*. 2004: Hong Kong Polytechnic University (Hong Kong).
- [96] Ceroni, F., M. Pecce, and S. Matthys, *Tension stiffening of reinforced concrete ties strengthened with externally bonded fiber-reinforced polymer sheets*. Journal of Composites for Construction, 2004. **8**(1): p. 22-32.
- [97] Kamiharako, A., T. Shimomura, and K. Maruyama, *The Influence of the substrate on the bond behavior of continuous fiber sheet*. Proceedings of the Japan Concrete Institute, 2003. **25**(2): p. 1735-1740.
- [98] Ren, H., *Study on basic theories and long time behavior of concrete structures strengthened by fiber reinforced polymers*. Dalian University of technology, 2003. **410**.
- [99] Dai, J.-G., Y. Sato, and T. Ueda, *Improving the load transfer and effective bond length for FRP composites bonded to concrete*. Proceedings of Japan Concrete Institute, 2002. **24**(2): p. 1423-8.
- [100] Faella, C., E. Martinelli, and E. Nigro, *Interface behaviour in FRP plates bonded to concrete: experimental tests and theoretical analyses*. 2003.
- [101] Nakaba, K., et al., *Bond behavior between fiber-reinforced polymer laminates and concrete*. Structural Journal, 2001. **98**(3): p. 359-367.
- [102] Tan, Z., *Experimental research for RC beam strengthened with GFRP*. Graduation thesis, Tsinghua Univ., Beijing, China (in Chinese), 2002.
- [103] Adhikary, B.B. and H. Mutsuyoshi. *Study on the bond between concrete and externally bonded CFRP sheet*. in *FRPRCS-5: Fibre-reinforced plastics for reinforced concrete structures Volume 1: Proceedings of the fifth international conference on fibre-reinforced plastics for reinforced concrete structures*, Cambridge, UK, 16-18 July 2001. 2001. Thomas Telford Publishing.
- [104] Kanakubo, T., et al., *Proposal for Local Bond Stress-Slip Relationship between FRP Sheet and Concrete*. Concr. Res. Technol. JCI, 2001. **12**: p. 33-43.
- [105] Yang, Y., Q. Yue, and Y. Hu, *Experimental study on bond performance between carbon fiber sheets and concrete*. Journal of building structures, 2001. **22**(3): p. 36-42.
- [106] Wu, Z., et al., *Experimental/analytical study on interfacial fracture energy and fracture propagation along FRP-concrete interface*. Special Publication, 2001. **201**: p. 133-152.

- [107] Yuan, H., Z. Wu, and H. Yoshizawa, *Theoretical solutions on interfacial stress transfer of externally bonded steel/composite laminates*. Doboku Gakkai Ronbunshu, 2001. **2001**(675): p. 27-39.
- [108] Maeda, T. *A study on bond mechanism of carbon fiber sheet*. in *Proceedings of third international symposium of non-metallic (FRP) reinforcement for concrete structures*. 1997.
- [109] Zhao, H., Y. Zhang, and M. Zhao. *Study on bond behavior of carbon fiber sheet and concrete base*. in *Chinese.] In Proc., 1st Chinese Academic Conf. on FRP-Concrete Structures*. 2000.
- [110] Tripi, J.M., et al., *Deformation in concrete with external CFRP sheet reinforcement*. Journal of Composites for Construction, 2000. **4**(2): p. 85-94.
- [111] Zhao, H., Y. Zhang, and M. Zhao. *Research on the bond performance between CFRP plate and concrete*. in *Proc., 1st Conf. on FRP Concrete Structures of China*. 2000.
- [112] Sato, Y., Y. ASANO, and T. Ueda, *Fundamental study on bond mechanism of carbon fiber sheet*. Doboku Gakkai Ronbunshu, 2000. **2000**(648): p. 71-87.
- [113] KAMIHARAKO, A., et al., *Analysis of bond and debonding behavior of continuous fiber sheet bonded on concrete*. Doboku Gakkai Ronbunshu, 1999. **1999**(634): p. 197-208.
- [114] Ueda, T., Y. Sato, and Y. Asano. *Experimental study on bond strength of continuous carbon fiber sheet*. in *4th International Symposium on Fiber Reinforced Polymer Reinforcement for Reinforced Concrete Structures*. 1999. American Concrete Institute.
- [115] Takeo, K., et al., *Bond characteristics of CFRP sheets in the CFRP bonding technique*. Proceedings of Japan concrete institute, 1997. **19**(2): p. 1599-1604.
- [116] Anderson, L.M., et al., *Introducing a series of methodological articles on considering complexity in systematic reviews of interventions*. Journal of clinical epidemiology, 2013. **66**(11): p. 1205-1208.
- [117] del Rey Castillo, E. and R. Kanitkar, *Effect of FRP spike anchor installation quality and concrete repair on the seismic behavior of FRP-strengthened RC columns*. Journal of Composites for Construction, 2021. **25**(1): p. 04020085.
- [118] del Rey Castillo, E., et al., *Digital image correlation (DIC) for measurement of strains and displacements in coarse, low volume-fraction FRP composites used in civil infrastructure*. Composite Structures, 2019. **212**: p. 43-57.
- [119] CNR, *Guide for the Design and Construction of Externally Bonded FRP Systems for Strengthening Existing Structures*. CNR-DT 200., 2013.
- [120] fib, *Externally applied FRP reinforcement for concrete structures*. 2019, Lausanne, Switzerland: FIB - International Federation for Structural Concrete.